ELSEVIER

Teaser We report how the understanding of SAR and the informed use of reliable data and models are pivotal to modulate the interplay with hERG channels.

Human ether-à-go-go-related potassium channel: exploring SAR to improve drug design

Maria Maddalena Cavalluzzi[1], Paola Imbrici[1], Roberta Gualdani[2], Angela Stefanachi[1], Giuseppe Felice Mangiatordi[3], Giovanni Lentini[1] and Orazio Nicolotti[1]

[1] Dipartimento di Farmacia - Scienze del Farmaco, Università degli Studi di Bari 'Aldo Moro', Via E. Orabona, 4, 70126 Bari, Italy
[2] Laboratory of Cell Physiology, Institute of Neuroscience, Université Catholique de Louvain, Brussels 1200, Belgium
[3] Istituto di Cristallografia, Consiglio Nazionale delle Ricerche, Via G. Amendola 122/O, 70126 Bari, Italy

hERG is best known as a primary anti-target, the inhibition of which is responsible for serious side effects. A renewed interest in hERG as a desired target, especially in oncology, was sparked because of its role in cellular proliferation and apoptosis. In this study, we survey the most recent advances regarding hERG by focusing on SAR in the attempt to elucidate, at a molecular level, off-target and on-target actions of potential hERG binders, which are highly promiscuous and largely varying in structure. Understanding the rationale behind hERG interactions and the molecular determinants of hERG activity is a real challenge and comprehension of this is of the utmost importance to prioritize compounds in early stages of drug discovery and to minimize cardiotoxicity attrition in preclinical and clinical studies.

Maria Maddalena Cavalluzzi graduated in chemistry and pharmaceutical technology with full honors in 1998 and obtained her PhD in drug sciences in 2002. She was then awarded with a 2-year postdoc and 4-year research grant in medicinal chemistry at the University of Bari (Italy). Currently, she is a research associate at the University of Bari. Her research activity is focused on antimyotonic and anticancer agent synthesis and resulted in 39 publications in international peer-reviewed journals.

Orazio Nicolotti graduated in chemistry and pharmaceutical technology with full honors in 1997 and received his PhD in drug sciences in 2001. He was then awarded with a 2-year postdoc at the University of Sheffield (UK) with a grant funded by GlaxoSmithKline. Since 2002, he is Professor of Medicinal Chemistry at the University of Bari (Italy). Major expertises in molecular and data modeling include: drug design; QSAR; predictive toxicology; combinatorial library design; evolutionary algorithms; docking and molecular dynamics. He is author of >100 research papers, eight book chapters, one international patent and 27 oral communications. He is also principal investigator of three research funded projects and supervisor of three industrial agreements for technology transfer.

Introduction

The human heart is a tireless organ that beats restlessly, with ~3 billion heartbeats per lifetime. The cardiac mechanical activity is characterized by two electrical phases (i.e., depolarization and repolarization) chasing each other cyclically. Such events rely on the finely tuned function of numerous voltage-gated ion channels. The cardiac Na^+ channel Nav1.5 and L-type Ca^{2+} channel Cav1.2 carry the major depolarizing currents, whereas a variety of K^+ channels are responsible for the repolarizing currents [1]. The electrical activity of the heart [2] is represented in the electrocardiogram (ECG), which includes: the P wave, reflecting atrial depolarization; the QRS complex, describing the ventricular depolarization; and the T wave, indicating the ventricular repolarization. The timespan between the beginning of the QRS complex and the end of the

Corresponding author: Nicolotti, O. (orazio.nicolotti@uniba.it)

https://doi.org/10.1016/j.drudis.2019.11.005

T wave is a crucial ECG feature and is known as the QT interval. This accounts for the ventricular action potential duration. Ether-à-go-go (EAG) K^+ channels (Kv10-12, as per the NC-IUPHAR guidelines) are a family of voltage-gated K^+ channels (VGKC or Kv) that have pivotal roles in the muscles, nervous system and heart. A subfamily of EAG, the EAG-related gene (ERG) K^+ channels, includes three isoforms (Kv11.1–11.3), with the human isoform Kv11.1 (commonly known as hERG) being coded by the gene *KCNH2*, as per the HUGO Gene Nomenclature Committee (HGNC) guidelines. Regardless of the preferred synonym (e.g., Kv11.1, hERG, HERG, hERG1, KCNH2, erg1, hergb), this K^+ channel is the leading actor of human cardiac repolarization [2]. In fact, the cardiac hERG channels are the main contributors to the rapidly activating delayed rectifier potassium current (IKr; hERG is also referred to as IKr channel [3]).

Congenital and drug-induced hERG dysfunctions can severely hamper the cardiac cycle. In particular, hERG blockers retard the cardiac repolarization thus prolonging the electrocardiographic QT interval. Abnormal prolongation of the QT interval – a pathological state commonly referred to as long QT syndrome (LQTS) – can, in turn, generate Torsades de Pointes (TdP), a sometimes fatal ventricular arrhythmia. The interest of medicinal chemists for hERG is basically related to drug-induced cardiotoxicity (off-target liability). In the past ten years, however, accumulated evidence suggested that hERG could be a target for a series of disorders. Besides the now mostly obsolete use of hERG-targeted class III antiarrhythmic drugs, hERG blockers have attracted an ever increasing interest as anticancer, chemosensitizer, diagnostic and prognostic agents [4]. hERG block could be intentionally pursued to cure rare short QT syndrome and muscle atrophy. Finally, hERG blockers can behave as chaperons and can restore the channel trafficking. Other hypothetical applications would address gut motility, neuronal, psychiatric, blood pressure and metabolic disorders. By contrast, hERG openers could be conveniently exploited as antidotes in the treatment of drug-induced and congenital LQTS, and to reduce electrical heterogeneity in the myocardium [4]. In the present article, we review the current knowledge on hERG structure and function by mostly focusing on SAR to identify the molecular determinants of hERG activity and, thus, to rationally address the design of better compounds. Details relating to our literature search (Table S1 and S2, see Supplementary material online) and valuable information concerning the interplay between hERG channel and tyrosine kinase inhibitors (Table S3, see Supplementary material online) are provided.

hERG channel structure and pathophysiology

Discovered in 1995, the hERG voltage-dependent K^+ channels are physiologically expressed in cardiac myocytes, neurons, smooth muscle of different organs and neuroendocrine cells [5,6]. The recent determination of the near-atomic resolution structure of hERG in an open conformation, using single-particle cryoelectron microscopy (cryo-EM) together with biophysical studies of channels expressed in heterologous systems, provided great insights into the molecular mechanism underlying hERG function and extreme sensitivity to drugs [7]. Like other K^+ channels, functional hERGs are tetramers formed by the co-assembly of four identical or highly similar α-subunits each containing six transmembrane α-helical segments (S1–S6). In each subunit, S1–S4 segments form the voltage sensing domain (VSD) and segments S5 and S6 contribute to the central pore-forming domain. Unlike classical voltage-gated K^+ channels, the VSD of each subunit is not domain-swapped, and thus interacts with the pore domain of the same subunit, whereas the cytoplasmic C-terminal domain presents a domain-swapped architecture [8]. The S5–S6 linker of each subunit contains typical residues that constitute the selectivity filter of K^+ channels (SVGFGNVS).

Importantly, in hERG the aromatic residue in the middle of the selectivity filter is a phenylalanine instead of a tyrosine as in most K^+ channels. The S6 segments line the central ion conducting pathway of the channel, and the cytoplasmic ends of each segment bend at a G648 gating hinge (the S6 bundle crossing) to form a narrow aperture (the activation gate) when the channel is closed. The S4 segment contains multiple positively charged amino acids that function as a primary voltage-sensing structure. In classical voltage-gated K^+ channels, in response to membrane depolarization, the S4 segments move outward and the attached cytoplasmic S4–S5 linker transfers the S4 movement to the S5–S6 segments favoring the opening of the activation gate (i.e., expansion of the S6 bundle crossing opening). Recent findings suggest that this electromechanical coupling occurs differently in hERG with respect to that observed for classical voltage-gated K^+ channels. hERG also presents a long NH_2 terminus located close to the bottom of the VSD that could participate to the slow deactivation kinetics of these channels. The C terminus encloses a cyclic nucleotide-binding domain. The unusually high sensitivity of hERG to many chemically different compounds can be at least in part accounted for by the peculiar features of the presumed drug-binding pore pocket, detailed through the cryo-EM resolution of hERG structure [8]. Drugs bind to the channel in the open or inactivated state. In each of the four subunits, two pore-lining aromatic residues: Y652 and F656, are crucial for drug binding as well as three residues at the bottom of the pore: T623, S624 and V625; and F557 in the S5 segment also contributes to the binding of some drugs. The putative negatively charged drug-binding cavity is located below the selectivity filter and, despite being atypically narrow, it is surrounded by four hydrophobic pockets that create a cavity large enough to accommodate substituted aromatic rings found in most high-affinity drugs [7]. Like other voltage-dependent K^+ channels, hERG can exist in closed, open and inactivated states but, in contrast to the vast majority of voltage-gated ion channels, hERG shows unusual kinetics. Indeed, the kinetics of activation and deactivation are much slower than the kinetics of inactivation and recovery from inactivation, which are very fast and voltage dependent. The peculiar gating kinetics account for some characteristic biophysical features of hERG (such as hooked tail currents) and underlie their distinct physiological role in cardiac repolarization [9].

In atrial and ventricular myocites, hERG represents the molecular counterpart sustaining IKr, a delayed rectifying K^+ current that contributes to determine the plateau and repolarization phase of cardiac action potential [6,10]. During the plateau, hERG channels are inactivated and enable proper calcium release and subsequent cardiac contraction. As membrane potential gradually repolarizes, hERG recovers from inactivation and generates an outward current that aids membrane full repolarization. Importantly, as a consequence of

the slow deactivation of hERG on returning to the closed state, IKr antagonizes cell depolarization if a premature ectopic beat occurs. Given the crucial role of hERG in cardiac physiology, it is not surprising that loss-of-function mutations in *KCNH2*, impairing channel gating or trafficking, cause congenital LQTS type 2.

The reduction of hERG activity in this disease retards cardiac repolarization and prolongs electrocardiographic QT interval leading to increased risk of developing serious ventricular cardiac arrhythmias, such as TdP and sudden death [8]. Drug-induced LQTS and fatal arrhythmias can also result from off-target inhibition of hERG, most commonly because some drugs block the channel pore. Among hERG blockers, there are structurally different molecules including antibiotics, antimalarials, gastroprokinetic agents, antihistamines, antiarrhythmics and antipsychotics. Therefore, hERG has been generally considered an undesirable pharmacological anti-target [9]. The LQTS was responsible for 30% of drugs withdrawn between 1990 and 2006 and, to date, at least 14 drugs have been withdrawn from the market because of QT prolongation and TdP risk [11]. Interestingly, hERG channels are often upregulated in neoplastic cell lines and primary human cancers, such as glioma, neural crest-derived tumors (neuroblastoma and melanoma) and a variety of carcinomas and leukemias; and cellular and molecular studies have demonstrated that hERG regulates different aspects of neoplastic progression [12]. Furthermore, preclinical studies indicate that hERG channel block has antineoplastic effects *in vivo*, thus supporting the perspective of hERG as a possible target for anticancer therapy, as long as hERG inhibitors do not produce cardiotoxic effects in humans.

SAR

hERG blockers are characterized by a basic group bridged to two flanking hydrophobic regions through flexible linkers. Based on this evidence, we designated two criteria to evaluate the strategies adopted to reduce the risk of off-target hERG toxicity, keeping the primary activity unbiased. The first consisted of monitoring the change in selectivity owing to the modulation of physicochemical properties (PCP) such as lipophilicity and basicity; the second criterion was to identify relationships between selectivity improvement and steric and electronic features (SEF). Ligand rigidification and π-stacking interaction hampering are the most commonly followed approaches. In this regard, we selected a pool of informative SAR after an extensive survey of the medicinal chemistry literature (from 2008 to 2018) to establish empirical guidelines aimed at minimizing unintentional hERG inhibitory activity (Tables 1 and 2, and Table S4, see Supplementary material online). Given the high number of case studies, only those reporting explicit IC_{50} values as a measure of hERG affinity are discussed herein. For the sake of clarity, we preferred to group the results according to the largest change of PCP and SEF although some structural modifications often affect both the criteria. In particular, we emphasize those structural variations increasing selectivity over hERG (estimated as the IC_{50hERG}:$IC_{50target}$ ratio) provided that the potency toward the desired target did not drop more than one order of magnitude (all the other cases are reported in the Supplementary material online).

Physicochemical properties

A strategy for decreasing hERG activity consists of lowering the lipophilicity of the ligand to prevent or, at least, reduce the occurrence of hydrophobic interactions at the binding pocket in the channel. In our analysis, we report only those analogs showing a log*P* variation ≥0.5 units, being known that clog*P* values are in the more optimistic cases affected by half an order of magnitude of error [13]. First, reducing the size of alkyl substituents could be a valuable option. For instance, replacing the ethyl substituent of the amide **1** with a methyl group of delta opioid receptor (DOR) agonists determined an eightfold decrease in hERG inhibitory activity (**2**) (Table 1) [14]. Slight reductions have also been reported in the series of C-C chemokine receptor type 2 (CCR2) antagonists (**3** and **4**) [15], where hERG affinity decreased proportionally to the log*P* reduction. Furthermore, lipophilicity can be reduced by adding polar atoms making H-bonding either as substituents of alkyl and aryl moieties {such as the hydroxyl group in the series of melanin concentrating hormone receptor 1 (MCHR1) antagonists **5**, **6** [16], CCR2 antagonists **7–10** [17], sodium channel blockers **11**, **12** [18] and (*RS*)-**13**, (*RS*)-**14** [19]} or one (or more) heteroatom(s) inserted into an aromatic ring thus leading to heteroaryl systems (such as pyridine **16** [20], pyrimidines **17** [20] and **20** [14], pyrazine **18** [20] and pyridazine **22** [21]). Noteworthy, this strategy is not always straightforward. In fact, when applied to a lead optimization program on CCR2 antagonists, the replacement of the left-hand phenyl ring of 4-azetidinyl-1-aryl cyclohexane **23** with the more polar pyridinyl ring (**24**) unexpectedly caused a drop in selectivity. Conversely, the insertion of a hydroxyl group at the 1-position of the cyclohexanyl ring of **24** led to approximately a ninefold increase of IC_{50} value (**25**) and the replacement with a pyrazinyl ring (**26**) led to a slightly wider selectivity window.

The best results for selectivity were obtained when hydroxyl (**27**) or amino (**28**) substituents were introduced into the pyridine ring of the 2-pyridyl regioisomer of **24** [22]. Afterwards in the same series of compounds, despite a different stereochemistry, the 5-thiazole group (**29**) was identified as the preferred left-end moiety, although the thiazole ring generally is not considered as a good alert for suppressing hERG *in vitro* activities [15]. The heteroatom insertion into an aliphatic ring was reported by Le Bourdonnec *et al*. [14] who observed more than one order of magnitude of log*P* drop and an 18-fold decreasing of hERG binding (**30**, **31**), along with a fivefold window over hERG, in their spirocyclic DOR agonist series. Notably, the lowering of pK_a and lipophilicity cooperated in reducing hERG inhibition when the piperidine ring of the CCR2 antagonist series was replaced by a morpholine one (**32**, **33**) [23]. In fact, a slightly milder effect was obtained by the insertion of a nitrogen atom (**34**), where this change lowered log*P* to about the same extent as the one observed with **33** and the corresponding pK_a value was reduced by about one order of magnitude [23].

Interestingly, the lipophilicity is also sensitive to bulky polar substituents that increase polar surface area (PSA). In a series of prolylcarboxypeptidase inhibitors, an ~10% increase in polarity in the biaryl region of the molecules attenuated hERG binding affinity by >100 times [24]. Moreover, the presence of highly polarized sulfonyl oxygen atoms led to a severe log*P* decrement, which is detrimental to hERG inhibition, in imidazole-based farnesyltransferase inhibitors (**35**, **36**) [25] and piperidin-4-yl urea derivatives showing MCHR1 antagonist activity (**37**, **38**) [26]. In the case of the bacterial topoisomerase inhibitors **39–42**, the PSA

TABLE 1

Synopsis of physicochemical properties (PCP) to minimize off-target hERG activity

Structure, target and main activity	Cpd no.	R (Ar, X)	hERG IC_{50} (μM)	Assay	clog *P*[a]	pK_a[b]	Primary target potency (nM)	Log (IC_{50hERG}/$IC_{50target}$)
			Decreasing alkyl substituent size					
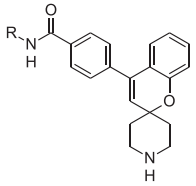	**1**	Et	12.0	Patch clamp	4.2		5.6	3.3
	2	Me	>100		3.7		18	3.7
DELTA OPIOID RECEPTOR (DOR) AGONISTS (analgesic agents) [14]								
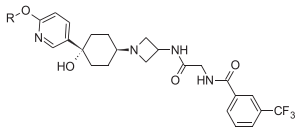	**3**	*t*Bu	5.5	[3H]astemizole binding assay	3.0		49	2.1
	4	*Et*	14.5		2.3		18	2.9
CHEMOKINE RECEPTOR CCR2 ANTAGONISTS (anti-inflammatory agents) [15]								
			Insertion of polar atoms					
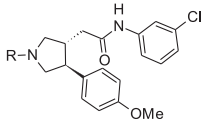	**5**	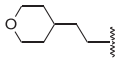	0.12	[3H]dofetilide binding assay	4.2		24	0.8
	6	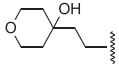	8.24		3.2		25	2.5
MELANIN-CONCENTRATING HORMONE RECEPTOR 1 (MCHR1) ANTAGONISTS (anti-obesity agents) [16]								
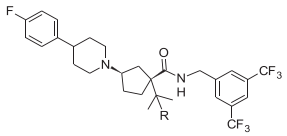	**7**	H	0.016	[35S]MK-0499 binding assay	6.5		3 ± 1	0.7
	8	OH	0.054		5.0		1.3 ± 0.49	1.6
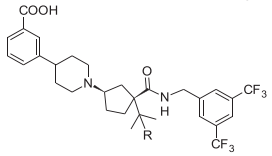	**9**	H	2.8		6.1		62 ± 4.9	1.6
	10	OH	19.7		4.6		45 ± 6.4	2.6
CHEMOKINE RECEPTOR CCR2 ANTAGONISTS (anti-inflammatory agents) [17]								

TABLE 1 (*Continued*)

Structure, target and main activity	Cpd no.	R (Ar, X)	hERG IC_{50} (μM)	Assay	clog *P*[a]	pK_a[b]	Primary target potency (nM)	Log (IC_{50hERG}/$IC_{50target}$)
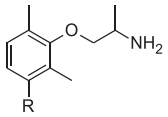	**11**	H	3.7 ± 0.7[c]	Patch clamp	0.53[d]		58 ± 13[e]	−1.2
	12	OH	22.4 ± 1.2[c]		0.02[d]		30 ± 3[e]	−0.1
hNav1.5 SODIUM CHANNEL BLOCKERS (antiarrhythmics) [97]								
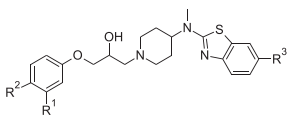	(*RS*)-**13**	$R^1 = R^2 = F$, $R^3 = H$	11.1 ± 0.4[f]	Patch clamp	4.7		1.7 ± 0.2[e]	0.8
	(*RS*)-**14**	$R^1 = R^3 = OH$, $R^2 = H$	55 ± 7[g]		3.2		≅ (*pers. commun.*)	~1.5
hNav1.4 SODIUM CHANNEL BLOCKERS (antimyotonic [98] and chemosensitizing agents [99])								
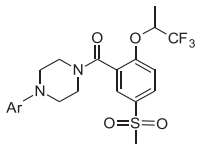	**15**	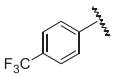	10	Patch clamp	3.5		30	2.5
	16	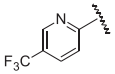	20		3.0		37	2.7
	17	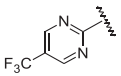	>40		2.6		100	>2.6
GLYCINE TRANSPORTER-1 (GlyT1) INHIBITORS (antischizophrenic agents) [20]	**18**	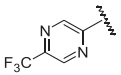	>40		2.9		110	>2.6
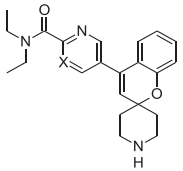	**19**	X = CH	44.1	Patch clamp	3.7		2.5	4.2
	20	X = N	>100		3.0		4.6	>4.3
DELTA OPIOID RECEPTOR (DOR) AGONISTS (analgesic agents) [14]								
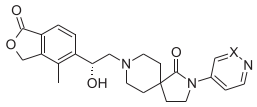	**21**	X = CH	10.4	[35S]MK-0499 binding assay	1.1	−0.4	64	2.2
	22	X = N	27.0				120	2.4
RENAL OUTER MEDULLARY POTASSIUM CHANNEL (ROMK) INHIBITORS (diuretic/ natriuretic agents) [21]								

TABLE 1 (*Continued*)

Structure, target and main activity	Cpd no.	R (Ar, X)	hERG IC_{50} (μM)	Assay	clog P^a	pK_a^b	Primary target potency (nM)	Log (IC_{50hERG}/$IC_{50target}$)
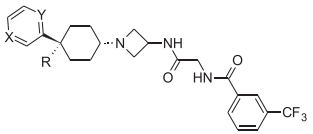	**23**	X = Y = CH, R = H	4.0	[3H]astemizole binding assay	4.3		35	2.1
	24	X = N, Y = CH, R = H	3.8		2.8		45	1.9
	25	X = N, Y = CH, R = OH	35		1.2		190	2.3
	26	X = Y = N, R = H	12		1.8		44	2.4
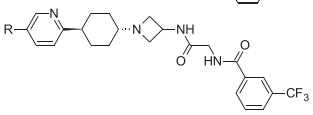	**27**	R = OH	10		2.8		13	2.9
	28	R = NH_2	37		2.1		85	2.6
CHEMOKINE RECEPTOR CCR2 ANTAGONISTS (anti-inflammatory agents) [22]								
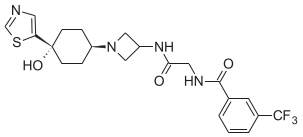	**29**		>50	[3H]astemizole binding assay	0.9		37	>3.1
CHEMOKINE RECEPTOR CCR2 ANTAGONISTS (anti-inflammatory agents) [15]								
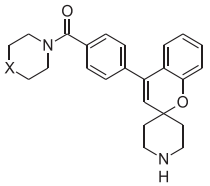	**30**	X = CH_2	3.0	Patch clamp	4.2	10.1	15	2.3
	31	X = O	54.2		2.7	10.1	50	3.0
DELTA OPIOID RECEPTOR (DOR) AGONISTS (analgesic agents) [14]								
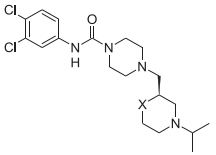	**32**	X = CH_2	1.3	Radioligand-binding assay	4.3	10.4	16	1.9
	33	X = O	6.3		3.1	7.7	17	2.6
	34	X = NH	5.6		3.3	9.0	26	2.3
CHEMOKINE RECEPTOR CCR2 ANTAGONISTS (anti-inflammatory agents) [23]								

TABLE 1 (*Continued*)

Structure, target and main activity	Cpd no.	R (Ar, X)	hERG IC_{50} (μM)	Assay	clog *P*[a]	pK_a[b]	Primary target potency (nM)	Log (IC_{50hERG}/$IC_{50target}$)
			Increasing polar surface area (PSA)					
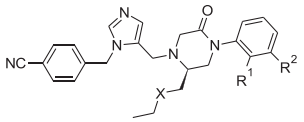	**35**	X = CH_2, R^1 = Me, R^2 = H	0.31	Voltage clamp	3.9 (PSA 65 $Å^2$)[b]		0.16	3.3
	36	X = SO_2, R^1 = H, R^2 = Cl	18		1.6 (PSA 108 $Å^2$)[b]		0.2	5.0
FARNESYLTRANSFERASE (FTase) INHIBITORS (antitumor agents) [25]								
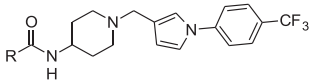	**37**	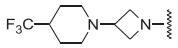	3.87	Patch clamp (IonWorks™)	4.3 (PSA 44 $Å^2$)[b]		81.8	1.7
MELANIN-CONCENTRATING HORMONE RECEPTOR 1 (MCHR1) ANTAGONISTS (antiobesity agents) [26]	**38**	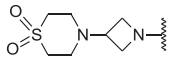	>31.6		1.7 (PSA 86 $Å^2$)[b]		99	>2.5
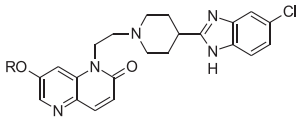	**39**		1	Medium-throughput electrophysiology IonWorks™ device	3.37[d] (PSA 64 $Å^2$)		250	0.6
	40	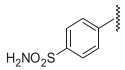	>33		4[d] (PSA 129 $Å^2$)		190	>2.2
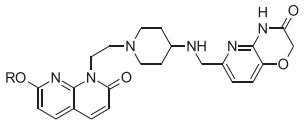	**41**		23		0.77[d] (PSA 106 $Å^2$)		250	2.0
	42	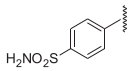	>100		0.71[d] (PSA 172 $Å^2$)		30	>3.5
Mycobacterium tuberculosis DNA GYRASE INHIBITORS (antituberculosis agents) [27]								
			Zwitterions					
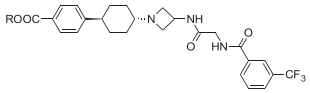	**43**	Me	1.3	[3H]astemizole binding assay	4.5[b]		80	1.2
	44	H	23.0		2.7[b]		70	2.5
CHEMOKINE RECEPTOR CCR2 ANTAGONISTS (anti-inflammatory agents) [22]								

TABLE 1 (*Continued*)

Structure, target and main activity	Cpd no.	R (Ar, X)		hERG IC_{50} (μM)	Assay	clog *P*[a]	pK_a[b]	Primary target potency (nM)	Log (IC_{50hERG}/$IC_{50target}$)
		R^1	R^2		Patch clamp				
	45		F	1.6		2.9[b]	10.7	28.8	1.7
	46		F	56		1.9[b]	5.1/10.7	27.5	3.3
	47	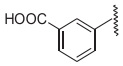	H	50		3.3[b]	3.7/10.7	26.3	3.3
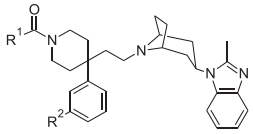	**48**		H	25		1.3[b]	4.1/10.7	7.4	3.5
	49		H	18		2.2[b]	4.5/10.7	45.7	2.6
CHEMOKINE RECEPTOR CCR5 ANTAGONISTS (anti-HIV agents) [28]	**50**	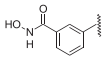	H	79		1.5[b]	8.7/10.7	25.1	3.5
			Decreasing basicity						
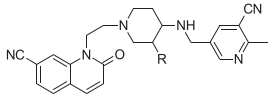	**51**	H		26	Medium-throughput	1.3[d]	8.2	0.06[h]	2.6[i]
	52	F (3*S*,4*R*)		>100	electrophysiology IonWorks™ device	1.29[d]	7.3	0.25[h]	>2.6[i]
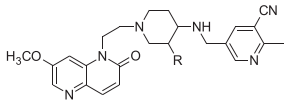	**53**	F (3*S*,4*R*)		90		1.29[d]	7.2	0.06[h]	3.2[i]
	54	OMe (3*S*,4*R*)		151		0.99[d]	8.1	0.06[h]	3.4[i]
Mycobacterium tuberculosis DNA GYRASE INHIBITORS (antituberculosis agents) [31]									
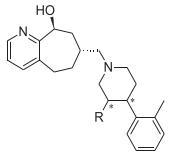	**(–)-55**	H		2.7 ± 0.34	[35S]MK-0499	3.1[d]	9.2[d]	4.5 ± 0.2	2.8
	56 (*trans*)	OH		40 ± 4	binding assay	2.2[d]	8.2[d]	10 ± 0	3.6
OPIOID RECEPTOR-LIKE 1 (ORL1) ANTAGONISTS (for CNS disorder treatment) [32]									

TABLE 1 (*Continued*)

Structure, target and main activity	Cpd no.	R (Ar, X)	hERG IC_{50} (μM)	Assay	clog *P*[a]	pK_a[b]	Primary target potency (nM)	Log (IC_{50hERG}/$IC_{50target}$)
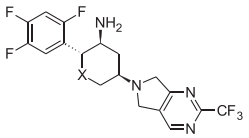	**57**	X = CH_2	4.8	Not reported	2.1	8.6[d]	0.5	4.0
	58	X = O	23		1.4	7.3[d]	1.3	4.2
DIPEPTIDYL PEPTIDASE 4 (DPP-4) INHIBITORS (for the treatment of type 2 diabetes mellitus) [33]								
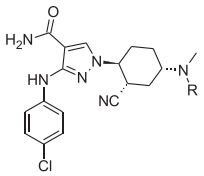	**59**	Me	12.2	[35S]MK-0499 binding assay	2.8	9.6	1.5	3.9
	60		46		4.2	8.2	0.6	4.9
JANUS KINASE 1 (JAK1) INHIBITORS (antirheumatic agents) [34]								
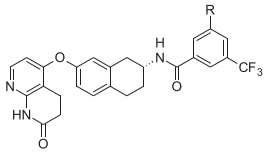	**61**		6.6 ± 3.1	Predictor™ hERG assay (Invitrogen)	4.8	8.6	2.9	3.4
	62	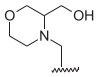	>100		5.0	5.2	4.0	>4.4
SERINE/THREONINE PROTEIN KINASE RAF INHIBITORS (anti-melanoma agents) [35]								
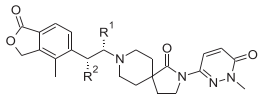	**63**	R^1 = R^2 = H	4.7	[35S]MK-0499 binding assay	–0.6	9.2	51	2.0
	64	R^1 = Me, R^2 = OH	>60		–0.3	8.6	42	>3.2
RENAL OUTER MEDULLARY POTASSIUM CHANNEL (ROMK) INHIBITORS (diuretic/ natriuretic agents) [21]								
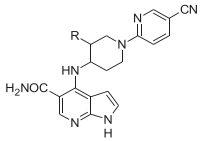	**65**	H	13.4	Rb efflux assay	3.4	7.0	1.3	4.0
	66	F (3*S*, 4*R*)	>100		3.0	7.0	0.30	>5.5
	67	F (3*R*, 4*S*)	>100		3.0	7.0	1.7	>4.8
JANUS KINASE 3 (JAK3) INHIBITORS (immunomodulators) [36]								

TABLE 1 (*Continued*)

Structure, target and main activity	Cpd no.	R (Ar, X)	hERG IC_{50} (μM)	Assay	clog P^{a}	pK_a^{b}	Primary target potency (nM)	Log (IC_{50hERG}/$IC_{50target}$)
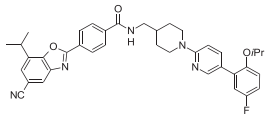	**68**		0.056	[35S]MK-0499 binding assay	6.2[b]	7.7	13	0.6
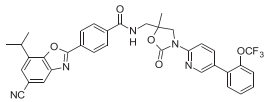	**69**		>30		6.9[b]	3.6	18–22	>3.1–3.2
CHOLESTERYL ESTER TRANSFER PROTEIN (CETP) INHIBITORS (antiatherogenic agents) [38]								

[a] cLog *P* values calculated with ACD/Labs Software, version 12.01.
[b] pK_a or log D values calculated with ACD/Labs Software, version 11.02 (SciFinder).
[c] Ref. [18].
[d] log D or pK_a values reported in the literature.
[e] IC_{50} values (μM) measured at 10 Hz stimulation frequencies.
[f] Ref. [19].
[g] Ref. [100].
[h] MIC values (μg/ml).
[i] log (IC_{50hERG}/MIC).

TABLE 2

Synopsis of stereoelectronic features (SEF) to minimize off-target hERG activity

Structure, target and main activity	Cpd no.	R (Ar, X, n)	hERG[a]	Assay	clog *P*[b]	Primary target activity (nM)	log (IC_{50hERG}/$IC_{50target}$)
		Electron-withdrawing substituent introduction					
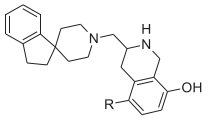	**70**	H	0.94	[3H]dofetilide	3.6	53.9	1.2
	71	Br	1.00	binding assay	4.5	35.1	1.4
	72	Cl	1.73		4.3	21.3	1.9
NOCICEPTIN/ORPHANIN FQ RECEPTOR ANTAGONISTS (for CNS disorder treatment) [41]							
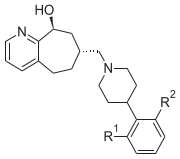	**(–)-73**	R^1 = Me, R^2 = H	2.7 ± 0.34	[35S]MK-0499	3.5	4.5 ± 0.2	2.8
	74	R^1 = Cl, R^2 = H	1.5 ± 0.17	binding assay	3.6	1.1 ± 0.1	3.1
	75	R^1 = R^2 = Cl	0.94 ± 0.22		4.2	0.47 ± 0.07	3.3
OPIOID RECEPTOR-LIKE 1 (ORL1) ANTAGONISTS (for CNS disorder treatment) [32]							
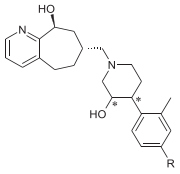	**76** (*trans*)	H	40 ± 4	[35S]MK-0499	2.2[c]	10 ± 0	3.6
	77 (*trans*)	F	13 ± 1.3	binding assay	2.5[c]	3.7 ± 0.1	3.5
OPIOID RECEPTOR-LIKE 1 (ORL1) ANTAGONISTS (for CNS disorder treatment) [32]							
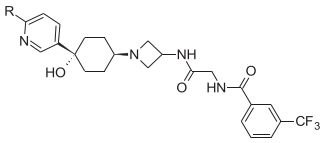	**78**	H	35.0	[3H]astemizole	1.2	190	2.3
	79	F	10.0	binding assay	1.3	190	1.7
CHEMOKINE RECEPTOR CCR2 ANTAGONISTS (anti-inflammatory agents) [15]							
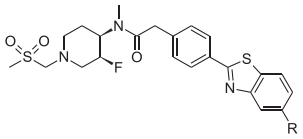	**80**	H	16	Patch clamp	2.1[c]	24	2.8
	81	F	7	(IonWorks™)	2.2[c]	18	2.6
GPR119 AGONISTS (for the treatment of type II diabetes) [42]							

TABLE 2 (*Continued*)

Structure, target and main activity	Cpd no.	R (Ar, X, n)	hERG[a]	Assay	clog *P*[b]	Primary target activity (nM)	log (IC_{50hERG}/$IC_{50target}$)
		Aryl moiety removal					
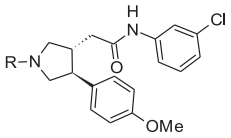	**82**	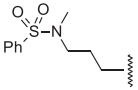	0.14	[3H]dofetilide binding assay	5.4	14	1.0
	83	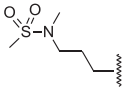	4.62		3.7	30	2.2
MELANIN-CONCENTRATING HORMONE RECEPTOR 1 (MCHR1) ANTAGONISTS (antiobesity agents) [16]							
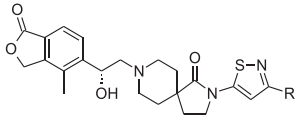	**84**	Ph	0.0095	[35S]MK-0499	2.9	340	−1.6
	85	Me	7.4	binding assay	1.6	18	2.6
RENAL OUTER MEDULLARY POTASSIUM CHANNEL (ROMK) INHIBITORS (diuretic/natriuretic agents) [21]							
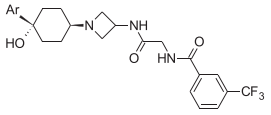	**86**	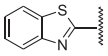	6.2	[3H]astemizole binding assay	3.2	16	2.6
	87		28		2.4	18	3.2
CHEMOKINE RECEPTOR CCR2 ANTAGONISTS (anti-inflammatory agents) [15]							
		Increasing Fsp^3 fraction					
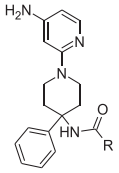	**88**		0.55[d]	[3H]dofetilide binding assay	2.2	60	1.0
	89		>10[d]		1.9	171	>1.8
δ-OPIOID RECEPTOR (DOR) AGONISTS (analgesic agents) [43]							
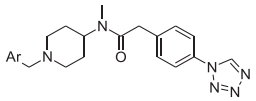	**90**	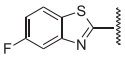	1.3	Patch clamp (IonWorks™)	2.9[c]	76	1.2
	91	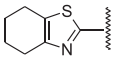	7.6		2.5[c]	396	1.3
GPR119 AGONISTS (for the treatment of type II diabetes) [42]							

TABLE 2 (*Continued*)

Structure, target and main activity	Cpd no.	R (Ar, X, n)	hERG[a]	Assay	clog *P*[b]	Primary target activity (nM)	log (IC_{50hERG}/$IC_{50target}$)
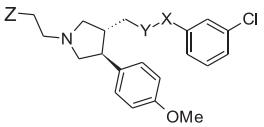	**92**	X = CO, Y = NH, Z = 4-methoxyphenyl	0.028	[3H]dofetilide	5.4	840	−1.5
	93	X = CO, Y = NH, Z = 4-pyranosyl	1.96	binding assay	4.1	350	0.8
	94	X = NH, Y = CO, Z = 3,4-dimethoxyphenyl	0.002		5.3	7	−0.5
	95	X = NH, Y = CO, Z = 4-pyranosyl	0.12		4.2	24	0.7
MELANIN-CONCENTRATING HORMONE RECEPTOR 1 (MCHR1) ANTAGONISTS (antiobesity agents) [16]							
		Rigidification					
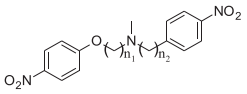	**96**	$n_1 = n_2 = 2$	5.7 ± 3.0[e]	[3H]astemizole	3.7		
	97	$n_1 = 2$, $n_2 = 1$	202 ± 49[e]	binding assay	3.6		
hERG BLOCKERS (pharmacological tools) [44]							
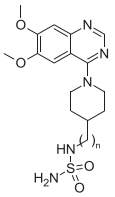	**98**	$n = 2$	0.601	[3H]dofetilide	0.46	36	1.2
	99	$n = 1$	>10	binding assay	0.14	61	>2.2
PLASMA CELL MEMBRANE PROTEIN-1 (PC-1) INHIBITORS (for the treatment of osteoarthritis) [45]							
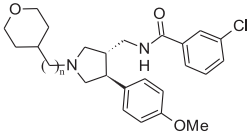	**100**	$n = 3$	1.03	[3H]dofetilide	4.8	310	0.5
	101	$n = 2$	1.96	binding assay	4.2	350	0.8
MELANIN-CONCENTRATING HORMONE RECEPTOR 1 (MCHR1) ANTAGONISTS (antiobesity agents) [16]							
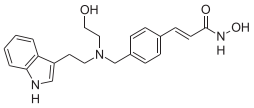	**102**		12.2	Patch clamp	3.4	9.0 ± 1.4	3.1
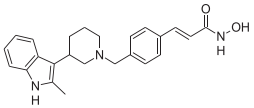	**103**		27.6		4.3	5.0 ± 1.2	3.7
HISTONE DEACETYLASE (HDAC) INHIBITORS (antitumor agents) [46]							

TABLE 2 (*Continued*)

Structure, target and main activity	Cpd no.	R (Ar, X, n)	hERG[a]	Assay	clog *P*[b]	Primary target activity (nM)	log (IC_{50hERG}/$IC_{50target}$)
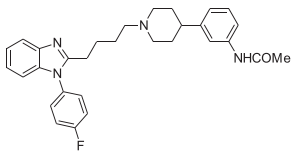	**104**		0.031	Patch clamp	5.8	0.6	1.7
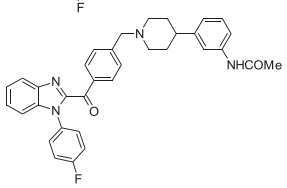	**105**		1.97		5.8	11	2.2
MELANIN-CONCENTRATING HORMONE RECEPTOR 1 (MCHR1) ANTAGONISTS (antiobesity agents) [47]		***Regioisomers***					
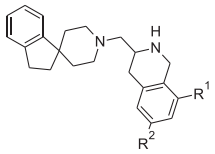	**106**	R^1 = H, R^2 = OH	0.34	[3H]dofetilide	3.6	227	0.2
	107	R^1 = OH, R^2 = H	0.94	binding assay	3.6	53.9	1.2
NOCICEPTIN/ORPHANIN FQ RECEPTOR ANTAGONISTS (for CNS disorder treatment) [41]							
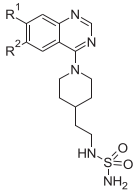	**108**	R^1 = Cl, R^2 = H	3.4	[3H]dofetilide	1.6[c]	>10[f]	−0.5
	109	R^1 = H, R^2 = Cl	5.42	binding assay	1.3	5.98[f]	−0.04
PLASMA CELL MEMBRANE PROTEIN-1 (PC-1) INHIBITORS (for the treatment of osteoarthritis) [45]							
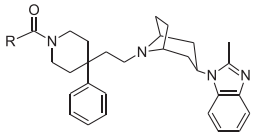	**110**	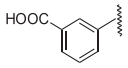	50	Patch clamp	3.3[g]	26.3	3.3
	111	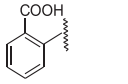	126		2.1[g]	30.9	3.6
CHEMOKINE RECEPTOR CCR5 ANTAGONISTS (anti-HIV agents) [28]							

[a] IC_{50} values (μM), unless otherwise indicated.
[b] clog *P* values calculated with ACD/Labs Software, version 12.01.
[c] log *D* values reported in the literature.
[d] K_i (μM).
[e] K_i (nM).
[f] μM.
[g] log *D* values calculated with ACD/Labs Software, version 11.02 (SciFinder).

effect mitigated the hERG liability despite similar log*P* values (**39** vs **40**; **41** vs **42**), thus demonstrating a greater influence of PSA than log*P* on hERG affinity [27]. Starting from the observation that the antihistamine terfenadine blocks hERG channels as opposed to its carboxylate metabolite fexofenadine, another fruitful way of tackling hERG-related liabilities is based on the introduction of an acidic moiety into an amine-containing ligand structure, thus leading to the formation of zwitterions showing significant log*D* variations with respect to the parent compound. Although several diverse examples of this approach can be found in the literature (e.g., CCR2 antagonists **43**, **44** [22] and CCR5 antagonists **46–50** [28]; see also Supplementary material online), zwitterions suffer from some drawbacks. They can have limited solubility at physiological pH [29], poor absorption and/or high *in vivo* clearance [28], and limited cellular membrane permeability [26]. Thus, despite the off-target hERG toxicity reduction, zwitterion introduction is not always an advisable strategy. It is well known that potency of hERG blockade is associated with the presence of basic nitrogen protonated at physiological pH and involved in key π-cation interactions with the channel. Therefore, another commonly used approach for reducing hERG affinity is to modulate the nitrogen pK_a. Electron-withdrawing substituents can be inserted near the basic center, with the fluorine atom being the most advisable choice because its relatively small size does not impair passive permeability [30].

A fourfold reduction of hERG inhibitory activity has been obtained when the fluorine atom was incorporated at the 3-position of the aminopiperidine moiety of *N*-linked aminopiperidine-based gyrase inhibitors (**51**, **52**) [31]. Furthermore, when the fluorine atom of the aminopiperidine **53** was replaced by a methoxy group [31], the albeit slightly improved hERG selectivity of the inhibitor **54** might stem from a reduced log*P* value and/or higher steric hindrance. Similarly, the opioid receptor-like 1 (ORL1) antagonist **56**, less basic and more polar than **55** [32], as well as the tetrahydropyran dipeptidyl peptidase IV (DPP IV) inhibitor **58**, isoster of **57** [33], showed a reduction of the hERG binding affinity owing to the sum of both the effects. It is also possible to limit the apparent basicity by increasing the steric hindrance around the basic nitrogen as demonstrated by the shielding induced by a methyl oxetane in the JAK1 inhibitor **60** [34] or by the nitrogen annulation as in the Raf inhibitor **62** [35]. It is worth noting that these modifications led to a lowering in hERG affinity despite the increased log*P* values, thus demonstrating the usefulness of this approach. By contrast, simple substitutions, such as a methyl and a hydroxyl group at the benzylic and homobenzylic positions, respectively, of the phenethylamine scaffold of some renal outer medullary potassium channel (ROMK) inhibitors (**63, 64**) led to a mitigation of hERG liability [21]. Interestingly, in the 1*H*-pyrrolo[2,3-*b*]pyridine-5-carboxamide series targeting JAK3 (**65–67**) [36], the insertion of a fluorine atom at the 3-position of the aminopiperidine moiety induced a sevenfold reduction in hERG inhibitory activity although no pK_a variation was observed. This result might stem from intramolecular electrostatic interactions (NH---F that reduce the H-bond donor character of the NH [37]. Notably, in this series the stereochemistry affected exclusively the main target but no difference in hERG affinity was observed. Finally, it is possible to completely remove the basicity transforming an amine group into a neutral function, as long as this modification has no effects on the primary on-target. For example, the piperidine moiety of the CETP inhibitor **68** has been replaced with an oxazolidinone ring (**69**) [38], whereas the well-known alkaloids brucine and strychnine have been transformed into their corresponding *N*-oxides [39]. As shown in Fig. 1, we have recently reported a neutral mexiletine-derived urea (MC450) which even behaves as a hERG agonist, thus showing a reversal of activity when compared with the basic parent compound mexiletine – a mild hERG blocker [40].

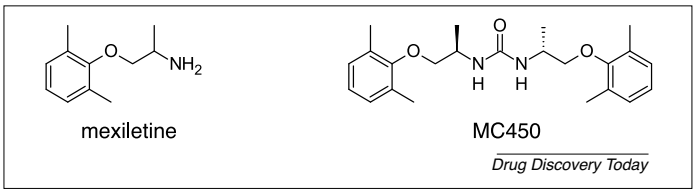

FIGURE 1

Neutral mexiletine-derived urea (MC450) behaves as a hERG agonist and shows a reversal of activity when compared with the basic parent compound mexiletine.

Stereoelectronic features

The reduction of aryl moiety electron density by incorporating electron-withdrawing or removing electron-donating groups is a fruitful strategy to hamper the drug-channel π-stacking interactions, despite the lipophilicity increase (Table 2). In a series of non-peptide antagonists of the nociceptin/orphanin FQ receptor, the hERG activity of the reference compound **70** was slightly affected only by the more electronegative chlorine (**72**) rather than bromide (**71**) [41]. By contrast, the introduction of a chlorine atom does not always guarantee a drop in hERG binding affinity as demonstrated by the series of ORL1 antagonists proposed by Yoshizumi *et al*. (**73–75**) where increased lipophilicity clearly plays a pivotal part in the interaction with the channel. Their selectivity over hERG, however, remained too high [32]. It is therefore extremely difficult to predict the effects resulting from the introduction of a chlorine atom on aryl moieties.

Despite the greatest electronegativity among the halogens, it seems that the fluorine atom introduced as a substituent at the aryl ring demonstrated to even improve the affinity for the channel (**76**, **77** [32]; **78**, **79** [15]; **80**, **81** [42]). This is probably due to the increased lipophilicity or to the ability of fluorine to reduce the energy of solvation and interact with polar groups (such as $-CO_2H$ and –OH) [37]. The removal of an aryl moiety, rather than the reduction of its electron density, is also advisable as demonstrated by the optimization strategies pursued by some pharmaceutical companies (for instance: the pyrrolidine MCHR1 antagonists **82**, **83** [16], spirocyclic ROMK inhibitors **84**, **85** [21] and 4-azetidinyl-1-aryl-cyclohexane CCR2 antagonists **86**, **87** [15]). In all the three reported cases, a key molecular determinant of hERG activity was removed and, moreover, a significant reduction of the log*P* value was observed (therefore, this case could also be quoted as a PCP effect). Furthermore, especially for compounds with molecular weight (MW) >450 Da, this approach allows reduction of MW and probably the design of compounds with more-adequate pharmacokinetics. Alternatively, the aryl moiety can be replaced by an

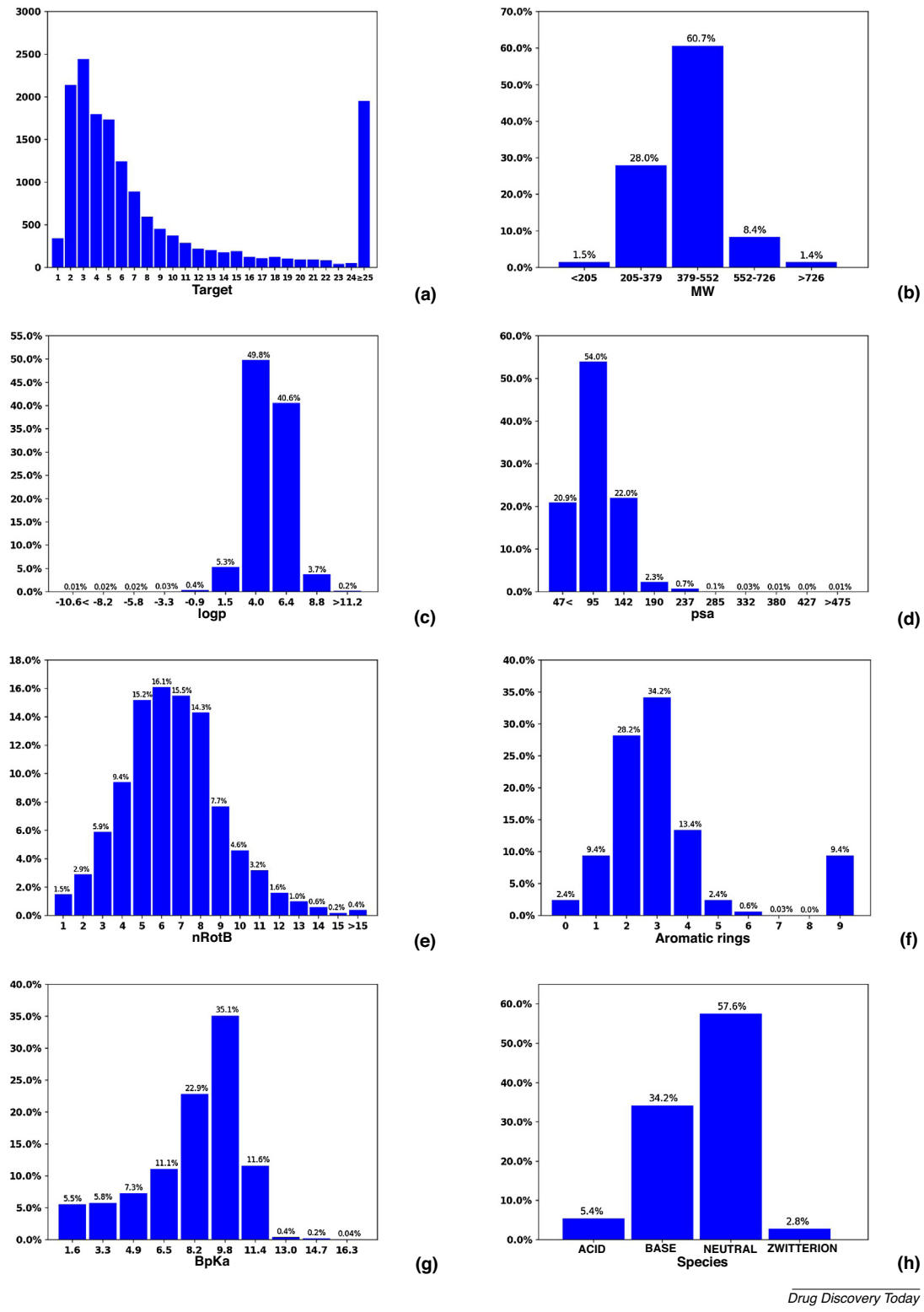

FIGURE 2

Distribution of some relevant features of small molecules biasing hERG taken from CHEMBL v.25 (target ID CHEMBL240) that are: **(a)** the number of targets; **(b)** molecular weight; **(c)** the log*P* values; **(d)** the value of the polar surface area; **(e)** the number of the rotatable bonds; **(f)** the number of the aromatic rings; **(g)** the pK_a values of base species; **(h)** the number of the species.

aliphatic ring, as successfully reported for the 2,4-diaminopyridine DOR agonists (**88**, **89**) [43], GPR119 agonists (**90**, **91**) [42] and pyrrolidine MCHR1 antagonists (**92–95**) [16].

In the last series, it is worth noting that the electron-withdrawing effect of the carbonyl joined to the right-end phenyl ring in the amides **92** and **93** is probably responsible for the reduced potency on hERG in comparison with the inverse amides **94** and **95**. Another viable strategy explored to mitigate hERG inhibition is the ligand rigidification. First, preference should be given to short and strained molecules. A shorter distance between one of the lipophilic end groups and the central nitrogen atom reduces hERG channel affinity as demonstrated in different series of compounds (dofetilide analogs **96**, **97** [44], quinazolin-4-piperidin-4′-alkyl sulfamide PC-1 inhibitors **98**, **99** [45] and pyrrolidine MCHR1 antagonists **100**, **101** [16]). Alternatively, the linker flexibility can be limited by replacing the alkyl chains with alkyl or aryl rings (hydroxamate-based histone deacetylase inhibitors **102**, **103** [46] and benzimidazole MCHR1 antagonists **104**, **105** [47], respectively). Finally, a slight difference in hERG affinity is sometimes observed for regioisomers (non-peptide antagonists of nociceptin/orphanin FQ receptor **106**, **107** [41], PC-1 inhibitors **108**, **109** [45] and 4,4-disubstituted piperidine-based CCR5 inhibitors **110**, **111** [28]) showing different binding modes.

Besides the SAR effects on hERG liability mitigation, the shift of selectivity toward the primary target must be carefully evaluated. In this respect, we observed that the most successfully affected classes of compounds include ligands of CCR2, MCHR1 and DOR. In particular, all the proposed structural modifications enhanced the selectivity window with the best results being obtained with 4-azetidin-1-yl-thiazole cyclohexane substitution (**23**, **29**) in the series of CCR2 antagonists. Moreover, the desired hERG IC_{50} standard (>30 μM) [33] was reached by the insertion of polar atoms capable of H-bonding (**25**, **28**). In the series of the pyrrolidine-based MCHR1 antagonists, the increase of Fsp^3 [13] led to compounds with high selectivity over hERG but where off-target affinity was still too high (**82**, **83**, **92–95**) [16]. Conversely, IC_{50} values >30 μM for hERG have been reached in the pyrrole series by reducing the log*P* value (**37**, **38**) [26]. In the spirocyclic DOR agonist series, reduced hERG affinity and higher selectivity for the primary target were obtained introducing heteroatoms (**19**, **20**, **30**, **31**) [14]. Another interesting observation is the PSA effect induced by the introduction of a sulfone group in FTase (**35**, **36**) [25] and *Mycobacterium tuberculosis* DNA gyrase (**40**, **42**) [27] inhibitors as well as in the MCHR1 antagonists (**37**, **38**) [26]. Finally, rewarding results have always been obtained through the modulation of pK_a, regardless of the involved primary target.

hERG data and models

Non-testing methods for the early prediction of hERG channel affinity of drug candidates are becoming increasingly important allowing significant savings in terms of money, time and, above all else, laboratory animals. In this respect, the recent increase of hERG blockage data provided by automated assays has helped in populating bioactivity chemical databases that represent a wealth of unprecedented information to derive trustable predictive models and to shed light on the molecular basis of hERG drug interactions.

High-quality hERG data

ChEMBL is a large collection of manually curated data for drug-like molecules including chemical, bioactivity and genomic information to address the design of new drugs. The latest release v.25 of the ChEMBL database released just in March 2019 contains >15 000 small molecules associated to hERG according to the target ID CHEMBL240 [48], the main features of which are depicted in Fig. 2.

At a first glimpse, small molecules associated to hERG show broad-binding poly-specificity as indicated by the spread in the number of targets; the tendency to have large MW and high hydrophobicity; the limited PSA; the preferred ranges of rotatable bonds from 5 to 8 and of aromatic rings from 2 to 3, respectively. Moreover, hERG inhibitors are normally neutral species or weak bases with pK_a values around 8. Although merely qualitative, this analysis indicates some relevant trends, which can be valuable for better understanding the SAR of hERG–drug interactions. To the best of our knowledge, an overview of representative curated hERG data collections so far used to derive *in silico* models, including reference databases and modeling datasets with no less than 100 compounds, is shown in Table S5 (see Supplementary material online). In addition, we herein review free online tools to predict hERG blockage that can be of practical use for assessing drug-induced QT syndrome. In this respect, an interesting recent investigation [49] describes the construction of a freely available integrated repository containing 9890 hERG inhibitors and 281 329 inactive small molecules. This database encompasses hERG-associated data entries retrieved from ChEMBL [48], GOSTAR [50], the NIH Chemical Genomics Center dataset registered in PubChem [51] and hERGCentral [52]. In particular, the database integration was obtained in several steps. More specifically, the formatting activity information implied the categorization in IC_{50}-type or inhibition-type data; the standardization of chemical structures involved the salt stripping; the filtering of non-drug-like compounds contemplated the removal of metal-containing molecules, compounds with MW < 150 or >700, compounds having <10 atoms and compounds with minor isotopes.

The classification of hERG inhibitors versus inactive compounds was made by considering as a threshold an $IC_{50} \leq 10$ μM or a percentage of inhibition ≥50 at 10 μM; in the case of large deviations of the assay experimental results probably owing to differences in the assay protocols or curation errors, outlier values were omitted and the majority vote-based strategy was followed to discern hERG inhibitors and inactive compounds. The structural diversity of the hERG inhibitors was assessed by employing the molecular frameworks conceived by Murko after analyzing large collections of known drugs [53]. Interestingly, the investigations of the physicochemical properties in the integrated database indicated that hERG inhibitors tend to have a larger MW (418.7 Da compared with 355.9 Da for inactive compounds), higher hydrophobicity according to Alog*P* and log*D* (3.80 and 3.22 compared with 2.77 and 2.58), have more cations (0.68 compared with 0.22) and more basic substituents (pK_a value of most basic substituents was 8.18 compared with 6.33). Although ~80% of the inactive compounds had no positively charged atoms, more than half of the hERG inhibitors contained at least one positively charged atom.

Predictive in silico *tools*

Among freely available tools, a milestone is the development of the Pred-hERG free online server enabling users to make predictions on the basis of binary/multiclass models and to draw probability maps catching different atomic contributions. Based on a large publicly available curated hERG dataset of 5984 compounds taken from ChEMBL, Pred-hERG makes predictions that are acceptable according to the OECD principles [54,55], thus avoiding the primary drawbacks of the majority of recently published QSAR studies for which, despite the innovativeness content, no proof of passing a y-randomization test and of the applicability domain (AD) [56] is provided. Another interesting tool is admetSAR [57], an open webserver for many endpoints based on a binary QSAR classification model for hERG blockage [58].

A transparent prediction of hERG blockers can also be made by checking for structural alerts whose usage is widely accepted in chemical toxicology and regulatory decision support. For instance, the tertiary amine is a well-defined flag for hERG blockage. In this respect, it should be said that, for a more informed and accurate safety assessment of new compounds, the structural alerts should be combined with rigorously validated QSAR models to minimize the tendency to disproportionally increase the number of false positives [56]. A mention to licensed software is also provided. The Cardiac Safety Simulator [59] can predict the blockage of multiple ion channels, including hERG [60]. Another commercial tool is the StarDrop module [61] implementing a hERG model to predict pIC_{50} values for inhibition of hERG expressed in mammalian cells. The StarDrop module allows the uploading of user data to improve the built-in model. Another commercial tool is QikProp (Schrödinger Suite) [62], designed to predict pIC_{50} values for inhibition of hERG expressed in mammalian cells. Based on the wealth of information from previous work, several SAR rules can be drawn to decrease toxicity of hERG blockers (Box 1).

Structure-based approaches

Ligand-based approaches show normally good performances when the predicted compounds have chemotypes not so dissimilar from those covered by a generally limited number of congeneric analogs belonging to the model training sets. Moreover, a prediction can be reliably accepted only if it falls within the model AD. This pitfall can be overcome by developing structure-based models. The latter capture, when available, the wealth of information on the protein-binding site and can be especially useful when the active compounds span different structural classes. Furthermore, structure-based models are provided with a much higher interpretability, thus properly meeting the stringent regulatory constraints [55]. Several research efforts have been made in the past years to shed light on the hERG–drug interactions and develop predictive structure-based models by means of computational approaches such as molecular docking and molecular dynamics (MD) simulations [63,64]. Of note is the paper by Anwar-Mohamed *et al.* [64] where a combined MD/docking-based model able to predict the hERG blockage of a panel of 18 compounds is presented. However, all these studies were performed on hERG homology models because, as said before, the near-atomic resolution structure of hERG has only recently been determined (PDB code: 5VA2 [7], resolution 3.8 Å; Fig. 3) by cryo-EM.

In particular, the templates employed to develop these models, namely other K^+ channels (i.e., Kir2.2, Kv1.2, KscA, KvaP and MthK), show a very low sequence similarity to hERG. Furthermore, most of the research efforts, based on long all-atom MD simulations [10], have been devoted to study the conformational changes occurring in the hERG central cavity (CC), hypothesized to be crucial for the drug binding [65] based on mutagenesis studies [66]. Nevertheless, an in-depth analysis of the cryo-EM structure revealed the presence of a peculiar CC in hERG [7], very different from those observed in the crystals of the K^+ channels used as templates, hence making us less confident about the trustworthiness of the published structural insights based on homology models. Despite that, no structure-based models have been developed so far, to the best of our knowledge, taking advantage of the cryo-EM structure. Efforts in this direction are represented by a co-authored paper [19] and two examples available in the literature [67,68]. Although of interest, these studies focus on single compounds already proved to be active on hERG, thus they do not provide any useful classification model for distinguishing unsafe from safe compounds. In this regard, it should be noted that deriving structure-based models is not free of risk. First, the resolution of the cryo-EM structure (3.8 Å) could be not sufficient for having an accurate picture from which informed conclusions are gained. A proper computational refinement is therefore mandatory before making such a 3D model suitable for structure-based approaches such as molecular docking.

Recently, Kotev *et al.* published the first proof-of-concept evidencing that cryo-EM structures can be efficiently exploited for structure-based investigations only if properly combined with 'state of the art' computational approaches accounting for protein flexibility, including long MD simulations, homology modeling and induced-fit molecular docking simulations [69]. In this respect, other interesting examples have been recently reported by Vaz *et al.* [70] and Helliwell *et al.* [71]. Second, hERG is not a mere pharmacological target but rather an anti-target responsible for important side-effects of many drugs used for noncardiovascular indications. In other words, a worthwhile structure-based model

BOX 1

Molecular determinants and recommended efficient strategies to reduce hERG affinity

- Lowering lipophilicity through site-specific structural changes (by decreasing alkyl substituent size, inserting heteroatoms or polar groups, PSA).
- Forming zwitterions (considering possible unwanted poor membrane permeability and oral bioavailability).
- Reducing basicity (by inserting electron-withdrawing substituents near the basic center, increasing the steric hindrance around the basic nitrogen, removing basic functionality).
- Reducing π-stacking interactions (by inserting electron-withdrawing substituents – excluding fluorine and CF_3 – on aryl moieties, removing peripheral aryl moieties, increasing Fsp^3 fraction).
- Reducing flexibility.

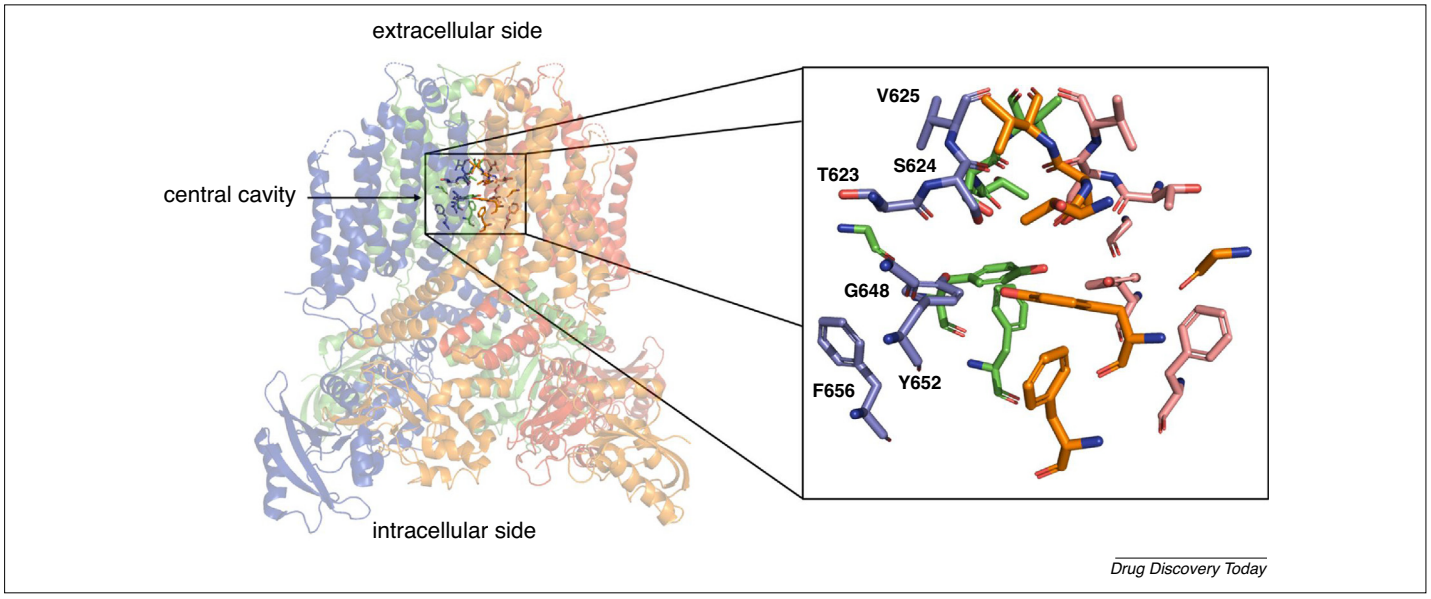

FIGURE 3

Cryo-EM structure of hERG tetramer (PDB code: 5VA2). Protein is represented as cartoons and each monomer is shown with a different color. All the residues forming the central cavity (T623, S624, V625, G648, Y652, F656) are represented as sticks. For the sake of clarity, residues referring to one monomer only are labeled in the magnified area.

should not be merely qualitative (as required in drug discovery programs) but rather quantitative, namely able to keep as low as possible the number of the so-called false negatives, namely active (unsafe) compounds incorrectly predicted as inactive (safe) [72,73]. Attention should be paid to adapt computational techniques commonly employed in drug discovery to the need of predictive toxicology. Although we are aware that the way for developing predictive structure-based models is not free of drawbacks, we do believe that it is a bet worth taking to meet the increasing need of preclinical cardiac safety assessment of drug candidates.

Testing screening methods

QT interval prolongation and hERG block play a prominent part in candidate selection during early drug discovery phases. Moreover, regulatory guidelines mandate that all drugs must be tested for hERG affinity and QT prolongation [74]. Conventional cardiac toxicity assays are performed with human embryonic kidney 293 (HEK 293) and Chinese hamster ovary (CHO) cells overexpressing the hERG channel. The IC_{50} value extrapolated for each compound is considered as an indication of possible QT interval prolongation. These preclinical tests can be subdivided into high-throughput assays, which enable the screening of large compound libraries, and lower throughput assays, which provide functional and mechanistic information about the interaction of drugs with the hERG channel. Within these methods, electrophysiological techniques enable control of membrane voltage and offer high time resolution. In particular, the patch clamp technique is employed to address questions such as the role of ionic currents in pathophysiology and to investigate the effects of newly developed drugs on ion channels. However, the patch clamp remains a low-efficiency procedure even for trained researchers. By contrast, radioligand-binding assays and fluorometric methods are useful for the initial screening of potential hERG interactions; but they do not provide control of membrane voltage and their results are influenced by other ion channels involved in resting membrane potential. For a comprehensive review the interested reader is referred elsewhere [75].

A recent article [76] shows an interesting combination of two techniques: patch clamp and atomic force microscopy, to simultaneously record membrane current and force development during contraction of isolated cardiomyocytes. Often, hERG channel tests have been considered non-physiological drug screening assays because they do not consider the fact that multiple ion channels, other than hERG, play a part in proarrhythmic risk [75]. For this reason, other tests, *ex vivo* and *in vivo*, are commonly used to assess QT prolongation. For example, action potential recordings, using extracellular microelectrodes, from Purkinje fibers, papillary muscle and isolated cardiomyocytes from guinea pig, rabbit or dog, are currently employed. A more complex assay, the arterially perfused ventricular wedge preparation, provides additional electrophysiological information about ECG parameters, early after depolarizations, delayed after depolarizations and AP triangulation. In addition, the Langendorff heart assay is a long-established technique that allows the examination of cardiac contractility and heart rate in isolated rat or rabbit heart perfused with the drug of interest.

Recently, the aforementioned techniques have been coupled with microfluidic-based technology [77] which offers the advantage of finely regulating fluid flow conditions (e.g., flow rate, shear stress and pulsatile flow) of drugs perfused. At the same time, microfluidics allow modification of the vessel geometry and the type of surface of the vessel walls, with the aim of mimicking ventricular cardiomyocyte physiology and 3D tissue-like architecture, and generating heart-on-a-chip structures [78].

Moreover, microfabrication-based patterning techniques have been employed to modulate the physiological and pathophysiological properties of cardiomyocytes. For example, the macroscopic cardiac tissue structure can be modified through surface topography [79] or different chemical composition of the adhesion surface [80].

To overcome the limitations of *in vitro* and *ex vivo* assays, several types of *in vivo* tests have been established. For example, the methoxamine-sensitized rabbit model and the chronic atrioventricular block dog model allow for the assessment of chronic exposure to drugs, drug metabolism and drug effects on sensitized hearts. Moreover, recent technical advances enabled recording of ECG parameters in conscious animals such as beagle dogs and monkeys [81]. However, these studies are expensive and ethically controversial. Therefore, they are only performed in the late drug discovery phases, immediately before clinical studies.

An interesting *in vivo* model used to assess cardiotoxicity is the Zebrafish, intensely studied for cardiac development, physiology and pathophysiology. A particular advantage is its morphological and functional similarity to the human heart. Because of the transparency of the early embryo, it is possible to directly observe drug effects on heart rate and rhythm. Moreover, Zebrafish are simple to breed, easy to modify genetically and they represent an alternative model for supporting the 3R guidelines: the refinement, reduction and replacement of animal studies (for a comprehensive review about the use of Zebrafish for cardiotoxicity assays see [82]). An overview of the methods used to assess proarrhythmic risk is shown in Table S6 (see Supplementary material online).

CiPA guidelines

The predictive value of the above approaches is still under debate, because the high sensitivity and, at the same time, low specificity of these assays might cause the exclusion from the market of potentially safe drugs that block the hERG channel but have little TdP risk [83]. This apparent anomaly can be explained by the multichannel pharmacological profile of these molecules, leading to complex alterations in the cardiac AP without translating into prolongation of the QT interval and TdP liability. This evidence suggests the inadequacy of the QT interval as a surrogate marker of actual proarrhythmic risk and the need for improved strategies to reduce failures in the drug discovery process [84].

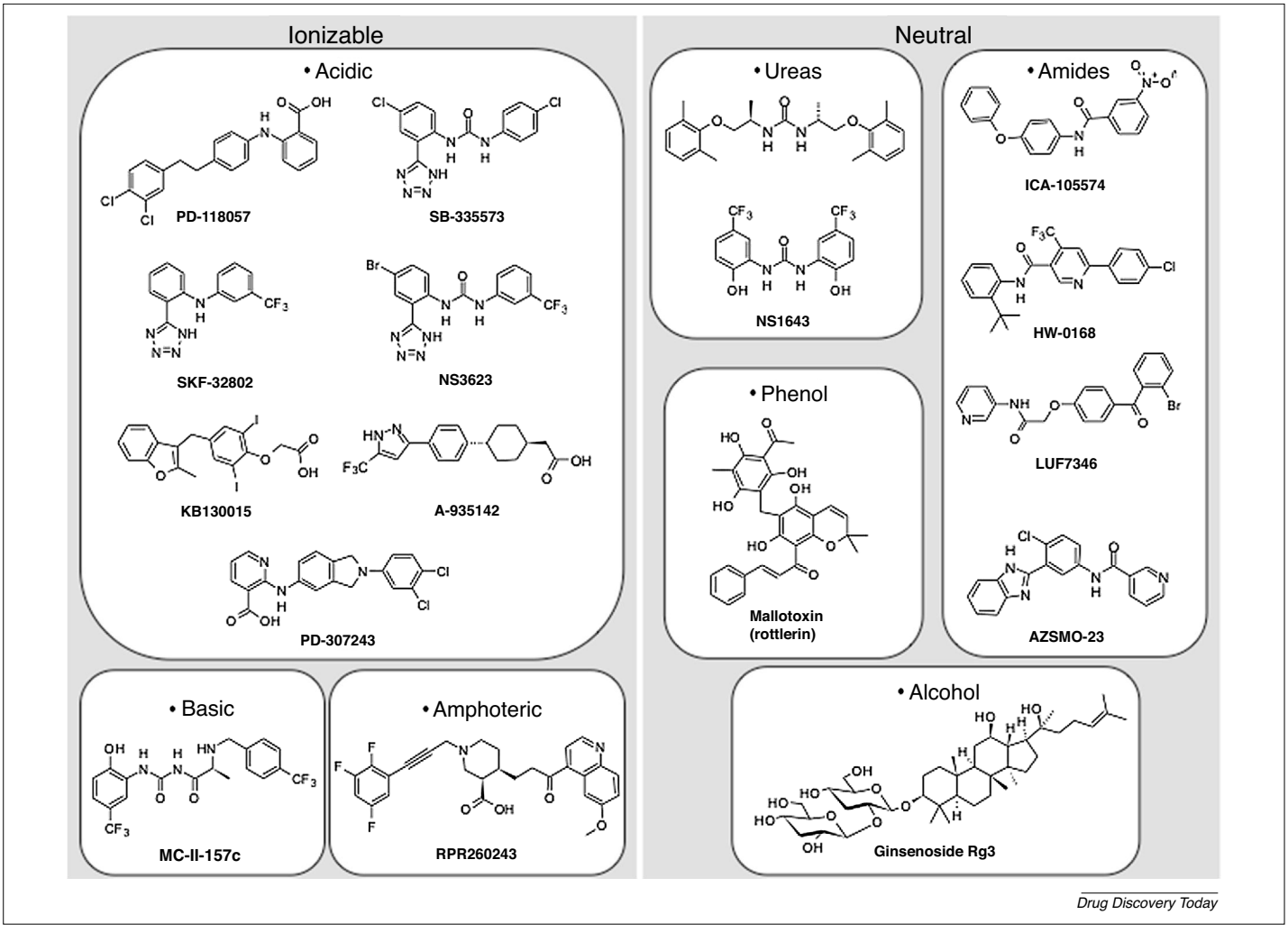

FIGURE 4

Representative structures of hERG openers grouped on the basis of the main functional groups and acid–base properties.

To address this concern, the FDA has proposed the comprehensive *in vitro* proarrhythmic assay (CiPA) [85]. CiPA requires: (i) assessing the potency and kinetics of block of hERG and other cardiac ion channels, using high-throughput *in vitro* screening; (ii) coupling this information with *in silico* models of the cardiac AP to assess integrated electrophysiological responses; (iii) verifying the predicted response in human induced pluripotent stem cell derived cardiomyocytes (hiPSC-CMs). hiPSC-CMs allow assessing the risk of drug-induced proarrhythmia using a human-derived model. Moreover, they offer the potential advantage to express a full range of ion channels as expressed in human ventricular myocytes. Finally, they can be differentiated to express normal but also many variant cardiac disease phenotypes, for example LQTS [86] and Timothy syndrome [87]. Several publications have shown the ability of hIPSC-CMs to detect proarrhythmic risk of drugs. The protocols and the techniques used to study hIPSCs for cardiac toxicity assessment are summarized in Table S7 (see Supplementary material online).

Small molecules as hERG activators

Despite hERG being mostly acknowledged as a primary anti-target, accumulated evidence indicates that small molecules as activators (also known as agonists, enhancers, openers) might have a role as antidotes to prevent drug-induced and congenital LQT syndromes and to limit electrical heterogeneity in the myocardium [88,89]. In this respect, a number of representative hERG activators [40,90–95] are shown in Fig. 4. As reported [90], hERG activators can be grouped into four classes on the basis of the prevalent mechanism behind the action potential duration (APD) shortening. More specifically: type 1 agonists impair deactivation; type 2 openers act primarily by attenuating inactivation; type 3 agonists shift the hERG channel opening to more negative potentials (hyperpolarizing shift); and type 4 enhancers increase the channel-opening probability. Based on channel symmetry, four identical putative binding sites exist whose multiple occupancy leads to APD shortening, although allosteric control could further complicate the scenario [94]. Noteworthy, even slight structural changes can affect the mechanisms of action (Fig. 4, by comparing SB-335573, type 4 agonist, and NS3623, type 2,4 opener [93]). The complex framework described above could explain why the SAR of hERG openers is still far from being well understood. For instance, stereoisomerism can be important for elucidating the SAR of openers whereas this topic s generally not so relevant for designing hERG blockers [19,96].

Concluding remarks

Despite the advances in the comprehension of hERG functioning and of its implications as an anti-target or even target, there are still unanswered questions. Just to name a few, it remains difficult to causatively relate, for instance, preclinical studies and the actual risk of TdS in humans because the relationships between hERG binding, LQTS and TdS is not yet fully understood. Next, state-dependence and kinetics of block introduce further complexity. Similar considerations hold on for pharmacokinetics. For example, norpropoxyphene, a major propoxyphene metabolite, shows only weak potency toward hERG. However, it can accumulate in cardiomyocytes determining severe cardiotoxicity. Drug interactions can even complicate the scenario. For instance, cisapride is more potent as a hERG blocker than sotalol. However, TdS occurs more in patients treated with sotalol because it is administered to patients with heart disorders whereas cisapride is normally taken by people with healthy hearts. Finally, a drug can induce proarrhythmic actions by interfering with hERG trafficking more than exerting a direct hERG blockade. Aware of the steep climb still in front of us, our intention here is to provide the reader with some rational medicinal chemistry rules to reduce the interference with hERG as a putative anti-target in drug design.

Conflicts of interest

The authors declare that there are no conflicts of interest regarding the publication of this article.

Appendix A. Supplementary data

Supplementary material related to this article can be found, in the online version, at doi:https://doi.org/10.1016/j.drudis.2019.11.005.

References

1 Rampe, D. and Brown, A.M. (2013) A history of the role of the hERG channel in cardiac risk assessment. *J. Pharmacol. Toxicol. Methods* 68, 13–22

2 Fermini, B. and Fossa, A.A. (2003) The impact of drug-induced QT interval prolongation on drug discovery and development. *Nat. Rev. Drug Discov.* 2, 439–447

3 Mitcheson, J.S. *et al.* (2000) Trapping of a methanesulfonanilide by closure of the HERG potassium channel activation gate. *J. Gen. Physiol.* 115, 229–240

4 Kratz, J.M. *et al.* (2017) Natural products modulating the hERG channel: heartaches and hope. *Nat. Prod. Rep.* 34, 957–980

5 Trudeau, M.C. *et al.* (1995) HERG, a human inward rectifier in the voltage-gated potassium channel family. *Science* 269, 92–95

6 Sanguinetti, M.C. *et al.* (1995) A mechanistic link between an inherited and an acquired cardiac arrhythmia: HERG encodes the IKr potassium channel. *Cell* 81, 299–307

7 Wang, W. and MacKinnon, R. (2017) Cryo-EM structure of the open human ether-à-go-go-related K+ channel hERG. *Cell* 169, 422–430

8 Vandenberg, J.I. *et al.* (2017) Towards a structural view of drug binding to hERG K+ channels. *Trends Pharmacol. Sci.* 38, 899–907

9 Vandenberg, J.I. *et al.* (2012) hERG K(+) channels: structure, function, and clinical significance. *Physiol. Rev.* 92, 1393–1478

10 Sanguinetti, M.C. and Tristani-Firouzi, M. (2006) hERG potassium channels and cardiac arrhythmia. *Nature* 440, 463–469

11 Stockbridge, N. *et al.* (2013) Dealing with global safety issues: was the response to QT-liability of non-cardiac drugs well coordinated? *Drug Saf.* 36, 167–182

12 Arcangeli, A. and Becchetti, A. (2017) hERG channels: from antitargets to novel targets for cancer therapy. *Clin. Cancer Res.* 23, 3–5

13 Cavalluzzi, M.M. *et al.* (2017) Ligand efficiency metrics in drug discovery: the pros and cons from a practical perspective. *Expert Opin. Drug Discov.* 12, 1087–1104

14 Le Bourdonnec, B. *et al.* (2009) Spirocyclic delta opioid receptor agonists for the treatment of pain: discovery of *N*,*N*-diethyl-3-hydroxy-4-(spiro[chromene-2,4′-piperidine]-4-yl) benzamide (ADL5747). *J. Med. Chem.* 52, 5685–5702

15 Zhang, X. *et al.* (2012) Discovery of a 4-azetidinyl-1-thiazoyl-cyclohexane CCR2 antagonist as a development candidate. *ACS Med. Chem. Lett.* 3, 1039–1044

16 Fox, B.M. *et al.* (2011) Novel pyrrolidine melanin-concentrating hormone receptor 1 antagonists with reduced hERG inhibition. *Bioorg. Med. Chem. Lett.* 21, 2460–2467

17 Pasternak, A. *et al.* (2008) Potent heteroarylpiperidine and carboxyphenylpiperidine 1-alkyl-cyclopentane carboxamide CCR2 antagonists. *Bioorg. Med. Chem. Lett.* 18, 994–998

18 Gualdani, R. *et al.* (2015) Inhibition of hERG potassium channel by the antiarrhythmic agent mexiletine and its metabolite m-hydroxymexiletine. *Pharmacol. Res. Perspect.* 3, e00160
19 Gualdani, R. *et al.* (2018) Molecular insights into hERG potassium channel blockade by lubeluzole. *Cell Physiol. Biochem.* 45, 2233–2245
20 Pinard, E. *et al.* (2010) Selective GlyT1 inhibitors: discovery of [4-(3-fluoro-5-trifluoromethylpyridin-2-yl)piperazin-1-yl][5-methanesulfonyl-2-((S)-2,2,2-trifluoro-1-methylethoxy)phenyl]methanone (RG1678), a promising novel medicine to treat schizophrenia. *J. Med. Chem.* 53, 4603–4614
21 Dong, S. *et al.* (2017) Improvement of hERG-ROMK index of spirocyclic ROMK inhibitors through scaffold optimization and incorporation of novel pharmacophores. *Bioorg. Med. Chem. Lett.* 27, 2559–2566
22 Zhang, X. *et al.* (2011) Overcoming hERG activity in the discovery of a series of 4-azetidinyl-1-aryl-cyclohexanes as CCR2 antagonists. *Bioorg. Med. Chem. Lett.* 21, 5577–5582
23 Cumming, J.G. *et al.* (2012) The design and synthesis of novel, potent and orally bioavailable *N*-aryl piperazine-1-carboxamide CCR2 antagonists with very high hERG selectivity. *Bioorg. Med. Chem. Lett.* 22, 3895–3899
24 Debenham, J.S. *et al.* (2013) Discovery and optimization of orally active cyclohexane-based prolylcarboxypeptidase (PrCP) inhibitors. *Bioorg. Med. Chem. Lett.* 23, 6228–6233
25 Bell, I.M. and Bilodeau, M.T. (2008) The Impact of IKr Blockade on Medicinal Chemistry Programs. *Curr. Top. Med. Chem.* http://www.eurekaselect.com/83111/article
26 Berglund, S. *et al.* (2009) Optimization of piperidin-4-yl-urea-containing melanin-concentrating hormone receptor 1 (MCH-R1) antagonists: reducing hERG-associated liabilities. *Bioorg. Med. Chem. Lett.* 19, 4274–4279
27 Hameed, P.S. *et al.* (2015) Left-hand side exploration of novel bacterial topoisomerase inhibitors to improve selectivity against hERG binding. *ACS Med. Chem. Lett.* 6, 741–746
28 Kazmierski, W.M. *et al.* (2011) Novel 4,4-disubstituted piperidine-based C-C chemokine receptor-5 inhibitors with high potency against human immunodeficiency virus-1 and an improved human ether-a-go-go related gene (hERG) profile. *J. Med. Chem.* 54, 3756–3767
29 Choi, Y.J. *et al.* (2014) Successful reduction of off-target hERG toxicity by structural modification of a T-type calcium channel blocker. *Bioorg. Med. Chem. Lett* 24, 880–883
30 Pettersson, M. *et al.* (2016) Quantitative assessment of the impact of fluorine substitution on P-glycoprotein (P-gp) mediated efflux, permeability, lipophilicity, and metabolic stability. *J. Med. Chem.* 59, 5284–5296
31 Hameed, P.S. *et al.* (2014) Novel N-linked aminopiperidine-based gyrase inhibitors with improved hERG and *in vivo* efficacy against *Mycobacterium tuberculosis*. *J. Med. Chem.* 57, 4889–4905
32 Yoshizumi, T. *et al.* (2008) A novel class of cycloalkano[b]pyridines as potent and orally active opioid receptor-like 1 antagonists with minimal binding affinity to the hERG K+ channel. *J. Med. Chem.* 51, 4021–4029
33 Biftu, T. *et al.* (2013) Novel tetrahydropyran analogs as dipeptidyl peptidase IV inhibitors: profile of clinical candidate (2R,3S,5R)-2-(2,5-difluorophenyl)-5-(4,6-dihydropyrrolo [3,4-c]pyrazol-5-(1H)-yl)tetrahydro-2H-pyran-3-amine (23) [corrected]. *Bioorg. Med. Chem. Lett.* 23, 5361–5366
34 Siu, T. *et al.* (2017) The discovery of 3-((4-chloro-3-methoxyphenyl)amino)-1-((3R,4S)-4-cyanotetrahydro-2H-pyran-3-yl)-1H-pyrazole-4-carboxamide, a highly ligand efficient and efficacious Janus kinase 1 selective inhibitor with favorable pharmacokinetic properties. *J. Med. Chem.* 60, 9676–9690
35 Huang, S.-C. *et al.* (2016) Optimization of tetrahydronaphthalene inhibitors of Raf with selectivity over hERG. *Bioorg. Med. Chem. Lett.* 26, 1156–1160
36 Nakajima, Y. *et al.* (2015) Synthesis and evaluation of novel 1H-pyrrolo[2,3-b] pyridine-5-carboxamide derivatives as potent and orally efficacious immunomodulators targeting JAK3. *Bioorg. Med. Chem.* 23, 4871–4883
37 Meanwell, N.A. (2018) Fluorine and fluorinated motifs in the design and application of bioisosteres for drug design. *J. Med. Chem.* 61, 5822–5880
38 Sweis, R.F. *et al.* (2011) 2-(4-Carbonylphenyl)benzoxazole inhibitors of CETP: attenuation of hERG binding and improved HDLc-raising efficacy. *Bioorg. Med. Chem. Lett.* 21, 2597–2600
39 Yuan, C. *et al.* (2018) Removal of hERG potassium channel affinity through introduction of an oxygen atom: molecular insights from structure-activity relationships of strychnine and its analogs. *Toxicol. Appl. Pharmacol.* 360, 109–119
40 Gualdani, R. *et al.* (2017) Discovery of a new mexiletine-derived agonist of the hERG K+ channel. *Biophys. Chem.* 229, 62–67
41 Hayashi, S. *et al.* (2016) Discovery of small-molecule nonpeptide antagonists of nociceptin/orphanin FQ receptor: the studies of design, synthesis, and structure–activity relationships for (4-arylpiperidine substituted-methyl)-[bicyclic (hetero) cycloalkanobenzene] derivatives. *Eur. J. Med. Chem* 114, 345–364
42 Brocklehurst, K.J. *et al.* (2011) Discovery, optimisation and *in vivo* evaluation of novel GPR119 agonists. *Bioorg. Med. Chem. Lett.* 21, 7310–7316
43 Owen, D.R. *et al.* (2009) 2,4-Diaminopyridine delta-opioid receptor agonists and their associated hERG pharmacology. *Bioorg. Med. Chem. Lett.* 19, 1702–1706
44 Shagufta, G.D. *et al.* (2009) Exploring chemical substructures essential for HERG k (+) channel blockade by synthesis and biological evaluation of dofetilide analogues. *ChemMedChem* 4, 1722–1732 order number 97000053126
45 Patel, S.D. *et al.* (2009) Quinazolin-4-piperidin-4-methyl sulfamide PC-1 inhibitors: alleviating hERG interactions through structure based design. *Bioorg. Med. Chem. Lett.* 19, 3339–3343
46 Cho, Y.S. *et al.* (2010) Conformational refinement of hydroxamate-based histone deacetylase inhibitors and exploration of 3-piperidin-3-ylindole analogues of dacinostat (LAQ824). *J. Med. Chem.* 53, 2952–2963
47 Sasmal, P.K. *et al.* (2011) Synthesis and SAR studies of benzimidazole derivatives as melanin concentrating hormone receptor 1 (MCHR1) antagonists: focus to detune hERG inhibition. *Med. Chem. Commun.* 2, 385–389
48 Gaulton, A. *et al.* (2012) ChEMBL: a large-scale bioactivity database for drug discovery. *Nucleic Acids Res.* 40 D1100–1107
49 Sato, T. *et al.* (2018) Construction of an integrated database for hERG blocking small molecules. *PLoS One* 13, e0199348
50 GVK BIO Online Structure Activity Relationship Database. Available at: https://gostardb.com/gostar/doc/Hyperlink%20Download%20PDF.pdf.
51 Kim, S. *et al.* (2016) PubChem substance and compound databases. *Nucleic Acids Res.* 44 D1202–1213
52 Du, F. *et al.* (2011) hERGCentral: a large database to store, retrieve, and analyze compound-human Ether-à-go-go related gene channel interactions to facilitate cardiotoxicity assessment in drug development. *Assay Drug Dev. Technol.* 9, 580–588
53 Bemis, G.W. and Murcko, M.A. (1996) The properties of known drugs. 1. Molecular frameworks. *J. Med. Chem.* 39, 2887–2893
54 Gissi, A. *et al.* (2014) An alternative QSAR-based approach for predicting the bioconcentration factor for regulatory purposes. *ALTEX* 31, 23–36
55 Nicolotti, O. *et al.* (2014) REACH and *in silico* methods: an attractive opportunity for medicinal chemists. *Drug Discov. Today* 19, 1757–1768
56 Alves, V. *et al.* (2016) Alarms about structural alerts. *Green Chem.* 18, 4348–4360
57 admetSAR. Available at: http://lmmd.ecust.edu.cn/admetsar1.
58 Shen, J. *et al.* (2010) Estimation of ADME properties with substructure pattern recognition. *J. Chem. Inf. Model.* 50, 1034–1041
59 Certara Cardiac Safety Simulator. Available at: https://www.certara.com/software/physiologically-based-pharmacokinetic-modeling-and-simulation/cardiac-safety-simulator/.
60 Wiśniowska, B. *et al.* (2015) Enhanced QSAR models for drug-triggered inhibition of the main cardiac ion currents. *J. Appl. Toxicol.* 35, 1030–1039
61 Optibrium – StarDrop. Available at: https://www.optibrium.com/stardrop/.
62 Schrödinger Release 2019-2: QikProp. Available at: https://www.schrodinger.com/.
63 Villoutreix, B.O. and Taboureau, O. (2015) Computational investigations of hERG channel blockers: new insights and current predictive models. *Adv. Drug Deliv. Rev.* 86, 72–82
64 Anwar-Mohamed, A. *et al.* (2014) A human ether-á-go-go-related (hERG) ion channel atomistic model generated by long supercomputer molecular dynamics simulations and its use in predicting drug cardiotoxicity. *Toxicol. Lett.* 230, 382–392
65 Fernandez, D. *et al.* (2004) Physicochemical features of the HERG channel drug binding site. *J. Biol. Chem.* 279, 10120–10127
66 Mitcheson, J.S. *et al.* (2000) A structural basis for drug-induced long QT syndrome. *PNAS* 97, 12329–12333
67 terbuleac, D. and Maniu, C.L. (2018) Computer simulations reveal a novel blocking mode of the hERG ion channel by the antiarrhythmic agent Clofilium. *Mol. Inf.* 37, e1700142
68 Kayık, G. *et al.* (2017) Structural investigation of vesnarinone at the pore domains of open and open-inactivated states of hERG1 K+ channel. *J. Mol. Graph. Model.* 77, 399–412
69 Kotev, M. *et al.* (2018) Pushing the limits of computational structure-based drug design with a Cryo-EM structure: the Ca2+ channel α2δ-1 subunit as a test case. *J. Chem. Inf. Model.* 58, 1707–1715
70 Vaz, R.J. *et al.* (2018) Molecular determinants of loperamide and *N*-desmethyl loperamide binding in the hERG cardiac K+ channel. *Bioorg. Med. Chem. Lett.* 28, 446–451
71 Helliwell, M.V. *et al.* (2018) Structural implications of hERG K+ channel block by a high-affinity minimally structured blocker. *J. Biol. Chem.* 293, 7040–7057
72 Trisciuzzi, D. *et al.* (2015) Docking-based classification models for exploratory toxicology studies on high-quality estrogenic experimental data. *Future Med. Chem.* 7, 1921–1936

73 Trisciuzzi, D. *et al.* (2017) Predictive structure-based toxicology approaches to assess the androgenic potential of chemicals. *J. Chem. Inf. Model.* 57, 2874–2884

74 ICH S7B note for guidance on the nonclinical evaluation of the potential for delayed ventricular repolarization (QT interval prolongation) by human pharmaceuticals. CHMP/ICH/423/02. https://database.ich.org/sites/default/files/S7B_Guideline.pdf.

75 Gintant, G. *et al.* (2016) Evolution of strategies to improve preclinical cardiac safety testing. *Nat. Rev. Drug Discov.* 15, 457–471

76 Ossola, D. *et al.* (2015) Force-controlled patch clamp of beating cardiac cells. *Nano Lett.* 15, 1743–1750

77 Su, X. *et al.* (2011) Microfluidic cell culture and its application in high-throughput drug screening: cardiotoxicity assay for hERG channels. *J. Biomol. Screen.* 16, 101–111

78 Agarwal, A. *et al.* (2013) Microfluidic heart on a chip for higher throughput pharmacological studies. *Lab Chip* 13, 3599–3608

79 Kim, D.-H. *et al.* (2010) Nanoscale cues regulate the structure and function of macroscopic cardiac tissue constructs. *PNAS* 107, 565–570

80 Agarwal, A. *et al.* (2013) Micropatterning alginate substrates for *in vitro* cardiovascular muscle on a chip. *Adv. Funct. Mater.* 23, 3738–3746

81 Derakhchan, K. *et al.* (2014) Detection of QTc interval prolongation using jacket telemetry in conscious non-human primates: comparison with implanted telemetry. *Br. J. Pharmacol.* 171, 509–522

82 Ravens, U. (2018) Ionic basis of cardiac electrophysiology in zebrafish compared to human hearts. *Prog. Biophys. Mol. Biol.* 138, 38–44

83 Polak, S. *et al.* (2015) Early drug discovery prediction of proarrhythmia potential and its covariates. *AAPS J.* 17, 1025–1032

84 Shah, R.R. (2005) Drug-induced QT interval prolongation—regulatory guidance and perspectives on hERG channel studies. *Novartis Found. Symp.* 266, 251–280 discussion 280–285

85 Sager, P.T. *et al.* (2014) Rechanneling the cardiac proarrhythmia safety paradigm: a meeting report from the Cardiac Safety Research Consortium. *Am. Heart J.* 167, 292–300

86 Moretti, A. *et al.* (2010) Patient-specific induced pluripotent stem-cell models for long-QT syndrome. *N. Eng. J. Med.* 363, 1397–1409

87 Yazawa, M. *et al.* (2011) Using induced pluripotent stem cells to investigate cardiac phenotypes in Timothy syndrome. *Nature* 471, 230–234

88 Wulff, H. *et al.* (2009) Voltage-gated potassium channels as therapeutic targets. *Nat. Rev. Drug Discov.* 8, 982–1001

89 Zhou, P. *et al.* (2011) Activation of human ether-a-go-go related gene (hERG) potassium channels by small molecules. *Acta Pharmacol. Sin.* 32, 781–788

90 Sanguinetti, M. (2014) HERG1 channel agonists and cardiac arrhythmia. *Curr. Opin. Pharmacol.* 15, 22–27. http://dx.doi.org/10.1016/j.coph.2013.11.006

91 Guo, J. *et al.* (2014) Structure driven design of novel human ether-a-go-go-related-gene channel (hERG1) activators. *PLoS One* 9, e105553

92 Dong, X. *et al.* (2019) Electrophysiological characterization of a small molecule activator on human ether-a-go-go-related gene (hERG) potassium channel. *J. Pharmacol. Sci.* 140, 284–290

93 Donovan, B.T. *et al.* (2018) Discovery and electrophysiological characterization of SKF-32802: a novel hERG agonist found through a large-scale structural similarity search. *Eur. J. Pharmacol.* 818, 306–327

94 Sala, L. *et al.* (2016) A new hERG allosteric modulator rescues genetic and drug-induced long-QT syndrome phenotypes in cardiomyocytes from isogenic pairs of patient induced pluripotent stem cells. *EMBO Mol. Med.* 8, 1065–1081

95 Mannikko, R. *et al.* (2015) Pharmacological and electrophysiological characterization of AZSMO-23, an activator of the hERG K(+) channel. *Br. J. Pharmacol.* 172, 3112–3125

96 Grilo, L.S. *et al.* (2010) Stereoselective inhibition of the hERG1 potassium channel. *Front. Pharmacol.* 1, 1–11. http://dx.doi.org/10.3389/fphar.2010.00137

97 Catalano, A. *et al.* (2012) An improved synthesis of m-hydroxymexiletine, a potent mexiletine metabolite. *Drug Metab. Lett.* . http://dx.doi.org/10.2174/1872312811206020124

98 Desaphy, J.-F. *et al.* (2013) Molecular dissection of lubeluzole use-dependent block of voltage-gated sodium channels discloses new therapeutic potentials. *Mol. Pharmacol.* 83, 406–415

99 Cavalluzzi, M.M. *et al.* (2013) A convenient synthesis of lubeluzole and its enantiomer: evaluation as chemosensitizing agents on human ovarian adenocarcinoma and lung carcinoma cells. *Bioorg. Med. Chem. Lett.* 23, 4820–4823

100 Gualdani, R. *et al.* (2015) Insights on molecular determinants of hERG K+ channel inhibition: design, synthesis, and biological evaluation of lubeluzole derivatives. *Biophys. J.* 108 582a